A study of electron-multiplying CCDs for use on the International X-ray Observatory off-plane x-ray grating spectrometer

A study of Electron-Multiplying CCDs for use on the International X-ray Observatory Off-Plane X-ray Grating Spectrometer

James H. Tutt[a*], Andrew D. Holland[a], Neil J. Murray[a], David J. Hall[a], Randall L. McEntaffer[b], James Endicott[c], Mark Robbins[c]
[a]Planetary and Space Sciences Research Institute, Open University, Milton Keynes, MK7 6AA, UK
[b]Department of Physics and Astronomy, University of Iowa, Iowa City, IA 52242-1479, USA
[c]e2v technologies plc, 106 Waterhouse Lane, Chelmsford, CM1 2QU, UK

ABSTRACT

CCDs are regularly used as imaging and spectroscopic devices on space telescopes at X-ray energies due to their high quantum efficiency and linearity across the energy range. The International X-ray Observatory's X-ray Grating Spectrometer will also look to make use of these devices across the energy band of 0.3 keV to 1 keV. At these energies, when photon counting, the charge generated in the silicon is close to the noise of the system. In order to be able to detect these low energy X-ray events, the system noise of the detector has to be minimised to have a sufficient signal-to-noise-ratio. By using an EM-CCD instead of a conventional CCD, any charge that is collected in the device can be multiplied before it is read out and as long as the EM-CCD is cool enough to adequately suppress the dark current, the signal-to-noise ratio of the device can be significantly increased, allowing soft X-ray events to be more easily detected.

This paper will look into the use of EM-CCDs for the detection of low energy X-rays, in particular the effect that using these devices will have on the signal to noise ratio as well as any degradation in resolution and FWHM that may occur due to the additional shot noise on the signal caused by the charge packet amplification process.

Keywords: IXO, OP-XGS, CCD, EM-CCD, L3, X-ray, FWHM, Excess noise factor.

1. INTRODUCTION

1.1 The International X-ray Observatory

The International X-ray Observatory (IXO) is a collaboration between ESA, NASA and JAXA and is a large scale mission under review in the ESA Cosmic Vision and NASA decadal survey. The telescope will be made up of a ~3 m^2 optic and have a focal length of 20 m with the main instrument focal plane sitting at the end of a deployable structure that is ~13 m in length. The telescope is due for launch in ~2022 and will be sent to a L2 halo orbit.

The Off-Plane X-ray Grating Spectrometer (OP-XGS) is a proposed instrument on IXO. It is planned to be a spectrometer that will cover the 0.3 keV to 1 keV energy range, have an effective area >1,000 cm^2 over this range and a resolution >3,000 ($\lambda/\Delta\lambda$). It will use a series of modules of off-plane gratings (grating grooves parallel to the direction of incoming radiation) to disperse 'soft' X-rays away from the main focus of the telescope onto a dedicated CCD camera array arranged in a conical pattern. The gratings will be housed on a tower and will extend 5.12 m from the focal plane creating a throw that is long enough to allow the X-rays to disperse over a large enough distance from the zero order to achieve the required resolution[1][2].

*j.h.tutt@open.ac.uk; tel: +44 (0)1908 655808; fax: +44 (0)1908 858022; http://www.open.ac.uk/cei

1.2 Electron-Multiplying CCDs (EM-CCDs)

EM-CCDs are traditionally used for optical applications, but their ability to increase the signal-to-noise ratio (SNR) of the charge collected in a device could have radical implications for use at X-ray energies on space instrumentation. When looking at low energy X-ray sources (< 0.4 keV), the Quantum Efficiency (QE) of even back-illuminated devices starts to rapidly fall off. As low energy X-ray events produce few electrons in their interactions with silicon, the system noise of the device can 'swamp' this signal and cause the X-ray photon to become indistinguishable from the noise.

Thus, by amplifying the charge packet generated by this incoming photon above the system noise of the device, the X-ray photon can be identified and used for scientific analysis. This paper aims to illustrate the potential of using of EM-CCDs in the detection of soft X-rays and to evaluate the possibility of using these devices on the OP-XGS.

2. THEORY

2.1 Quantum efficiency, filters and readout speed

Back-illuminated CCDs are frequently used to detect X-rays in the 0.3 keV to 1 keV energy range due to their higher Quantum efficiency (QE) than front-illuminated devices and this is the energy range that the OP-XGS will be working at. Figure 1 shows a plot of the modelled QE of the back-illuminated CCDs used on the Reflection Grating Spectrometer (RGS) on XMM-Newton. At the lowest energies considered by this instrument, it can be seen that the QE drops off very quickly with decreasing energy (solid line). This is especially the case when the detector employs a stray light filter for optical photon rejection (dashed line).

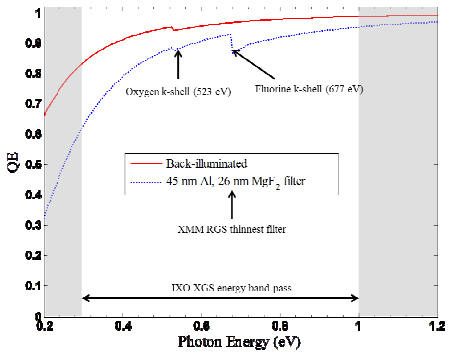

Figure 1. The modeled QE of the back-illuminated CCDs used on the RGS. The solid line shows the QE of the device and the dashed line shows how the QE reduces by employing an optical blocking filter. The filter thickness shown is the thinnest filter used on the RGS. The k-shell absorption edges are indicated for oxygen and fluorine.

The QE falls away quickly at low energies (<0.4 keV) as the incoming X-rays do not have enough energy to penetrate the native oxide/filters and dead layer of the CCD and so the interaction between the X-rays and the silicon occurs in a part of the device that does not lead to the electrons being collected in the active silicon. The lower the energy, the less material that the X-ray can pass through and so there is a higher probability that the X-ray will not be detected leading to a drop in QE. Increasing the amount of material the X-rays need to travel through (in a filter), reduces this probability of detecting an X-ray interaction and so the QE falls further still.

Space instruments working in the X-ray band often require optical blocking filters to reduce unwanted stray light incident on the detectors. However, by adding a filter layer onto the device, the amount of 'dead' material that the incident X-ray has to penetrate in order to be detected in the active silicon is increased and so the QE at low energies reduces even further. If the detector can be read out and refreshed at a faster rate, the stray light background signal incident, with a constant number of photons per pixel per second, will be reduced on a frame-by-frame basis. This may allow for use a thinner filter, whilst maintaining the same acceptable level of stray light, hence yielding a better QE at lower energies. However, reading out a CCD faster causes increased system noise and hence a degradation in the signal-to-noise ratio (SNR), resulting in a loss of sensitivity of the device to small signals such as those generated by soft X-rays. By using an EM-CCD, gain on the photo-generated signal can be applied to restore or improve the SNR at fast readout rates, however the charge amplification process introduces an increased noise on the signal for the device which varies with gain and may adversely affect the spectroscopic performance of the device.

Figure 2 shows a classic example of a 'banana plot' captured by the Reflection Grating Spectrometer (RGS) instrument on XMM-Newton. The three clearly resolved curves are created by the dispersed light incident on the CCD array in orders 1st through 3rd. In the 1st order, at low energies the charge detected by incident photons starts to be incorporated into the noise of the device and so are harder to resolve and because of this the RGS has a low energy cut-off of 0.33 keV[3].

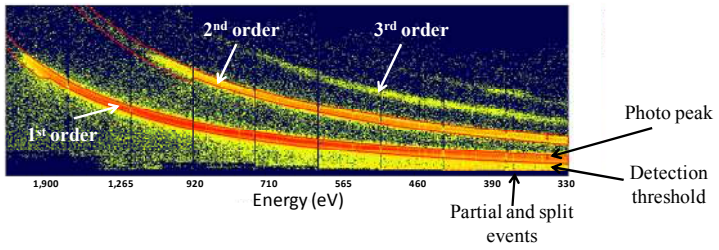

Figure 2. Energy vs. position plot for the XMM RGS camera array showing multiple orders demonstrating relatively low SNR for low energy photons.

If an EM-CCD was used instead of a conventional CCD, each of the curves would effectively have a positive translation in the y-axis of Figure 3, whilst the noise floor remaining at the same location. This would give a much improved SNR and thus make the softer X-ray photons (<0.4 keV) easier to detect and increase the possible bandpass of the instrument to 0.2 keV.

2.2 Electron Multiplying Charge-Coupled Devices (EM-CCDs)

An EM-CCD is constructed using a standard CCD structure which has a multiplication register placed after the serial readout register and before the output amplifier (Figure 3). This means that the signal on the chip can be amplified before the signal is affected by the readout noise which, when a device is run cold (< -80°C), is the dominant source of system noise at low signal.

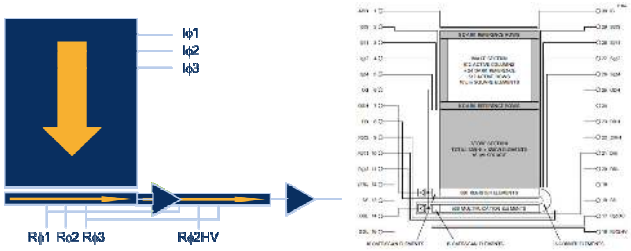

Figure 3. EM-CCD shown with parallel clocks (Iφ), serial clocks (Rφ) and High Voltage clocks (RφHV) on the left and the schematic of the CCD97 that was used for this work on the right[4].

The multiplication register works by accelerating charge packets in the serial register through areas of high potential. The electrons in the charge packet can then ionise silicon atoms in the device through impact ionisation, thus increasing the number of electrons in the signal. The probability of impact ionisation taking place for each electron at each register is low and is given by a factor *g*, but if this process is repeated through the multiplication register through *N* gain register elements the total gain of the system, *G*, is given by:

$$G = (1 + g)^N$$

Changing the voltage on the electrodes in the multiplication register changes the gain of the system. A higher voltage leads to a higher probability of impact ionisation taking place and so the device has a higher gain provided it has the same number of multiplication elements, *N*. This gain-voltage relationship can then be calibrated and so, for a given voltage, a prediction of the expected level of gain is possible and is shown in Figure 4.

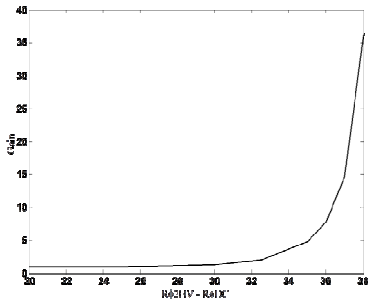

Figure 4. Gain vs. Voltage for an e2v CCD97 operating at -120°C.

2.2.1 Detection of X-rays with EM-CCDs

EM-CCDs are usually used at optical wavelengths as with a gain of 1 the shot noise on the signal is equal to (1 x shot noise), the increase in this shot noise due an addition of a multiplication register only leads to a doubling of the shot noise (see section 2.2.2). For X-ray photons multiple electron-hole pairs are produced as the quantity depends on the energy of the incident photon. When an X-ray photon interacts with the silicon, the electron released moves through the silicon and, depending on its energy, causes another electron to be released through photo-ionisation. This ionisation avalanche continues until the energy of the released electrons falls below that of the band gap of a silicon atom, creating a charge cloud of electrons[5].

The uncertainty in the number of electrons produced is equal to the square root of the mean number of electrons and so is high for large signals. Hence, the number of electrons generated forms a Poisson distribution around the mean number of electrons. However, this is not entirely true for silicon at X-ray energies as the Fano factor also has to be taken into account. Poisson statistics does not take into account that the production of the electrons in this charge cloud is not an independent process, therefore the variance is much smaller than would be expected in a purely Poisson process. The ratio of the variance to the prediction made by Poisson statistics is denoted by the Fano facto (f)[6]. This factor alters the statistics of the shot noise on the electron-hole production, allowing a better noise result. The shot noise for an X-ray detected in silicon is smaller than the square root of the number of generated electron-hole pairs. This means that the shot noise on the signal is equal to (f x shot noise) = (0.115 x shot noise)

The second component of shot noise, generated by the gain in signal in the multiplication register, is unaffected by the Fano factor and so there is still an increase in the shot noise due to the signal amplification. This noise is the same per electron as in the optical case. It is predicted that you increase the multiplication on your shot noise by a factor of ~10 from 0.115 without a multiplication register to 1.115 with the register and so using an EMCCD with X-rays causes a larger FWHM degradation than in the optical case.

2.2.2 Excess noise factor

For optical wavelengths, as the multiplication of the shot noise only doubles through the introduction of a multiplication register it has a small impact on the total noise. The relationship between the shot noise on the signal before and after multiplication is known as the excess noise factor (F) and is well understood. (Figure 5) [7].

At high gains, the effect of this excess noise tends to 2, but at gains of less than ~10, the effect drops rapidly towards 1 for a gain of 1. In general,

$$F = (2G + g - 1) / G(1 + g)$$

Therefore, if the device is operated at low gain (<10), the combined effect of the two components of shot noise is lower than that operating at higher gain. Applying this knowledge to the detection of X-rays, a lower gain environment could produce X-ray peaks with a narrower FWHM and so help achieve the order separation requirement of the OP-XGS, discussed in Section 2.3.

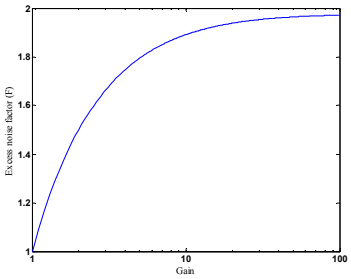

Figure 5. Plot showing the change in the excess noise factor (F) with varying gain.

2.2.3 Excess noise factor with X-rays

In order to try and predict the effect of using EM-CCDs to detect X-rays at low and high gains, a Monte Carlo model was developed to model its behaviour. A flat field image of 82 electrons per pixel was created (~300 eV for an EM-CCD cooled to -100 °C) and then each pixel was given a Fano factor adjusted Poisson distribution. A flat field was used in order to generate a statistically significant data set quickly. The electrons in each simulated pixel were run through the multiplication register and by comparing the variance on the input electrons and output electrons as well as knowing the gain of the system, it was possible to produce a theoretical plot of the excess noise factor at different levels of gain. This model could then be tested by using it to predict the behaviour of optical photons being detected and plotting the theoretical model to see how it coincided with the points. This comparison is shown in Figure 6.

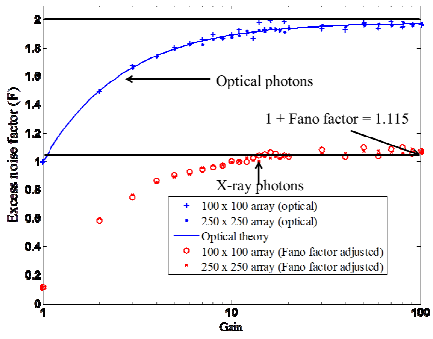

Figure 6. Plot showing the data obtained from the Monte Carlo model in an EM-CCD for X-rays (Fano factor adjusted and excess noise – bottom line) and optical photons (top line). The theoretical model for optical photons is also shown.

The consistency of the model and theory in the case of optical photons allowed a trend for X-ray photons (Fano factor adjusted) to be constrained and predicted. Although this required verification through experimental testing, if confirmed, it would show the presence of a low noise, low gain region that the device could be operated in to better achieve the order separation requirement. The model and mathematical prediction for the excess noise factor in X-rays, or "modified noise factor", shows that it should tend to 1 + Fano factor, or 1.115 at high avalanche multiplication gains.

2.3 Order separation requirement

As discussed, the OP-XGS is planned to have a resolution of >3,000 across the energy range 0.3 keV – 1 kev. In order to achieve this, the OP-XGS will have to use several orders of dispersion[8]. The different orders of dispersed light are superimposed on the CCD array creating individual arcs per grating module. The minimum size of energetic separation between photons incident at the same physical location on the detector will be ~200 eV, as shown in Figure 7. Due to this effect, the CCD must be able to discriminate between photo-peaks of 200 eV separations across the instrument bandpass 0.3 keV to 1.0 keV.

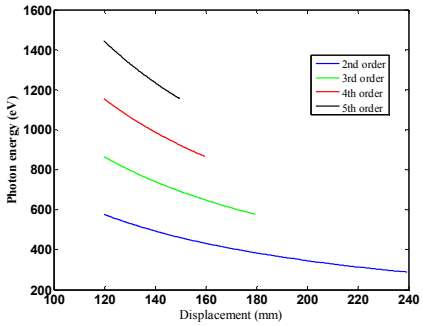

Figure 7. Photon energy vs. displacement on the focal plane array for 2nd – 5th order reflection. It shows the minimum energy separation between the orders occurring at the same position and so sets an order separation requirement on the detector.

For a conventional CCD, if the readout noise of the device is optimised, this separation is easily achievable and has been demonstrated. For an EM-CCD, an extra component of shot noise is introduced by the charge avalanche multiplication process and may cause degradation in the FWHM of the device and so it is possible that the requirement will be harder to achieve. If at low gain the total shot noise found with the device follows the same trend as found with optical detection then it should be possible to minimise the FWHM by running the EM-CCD at low gain. The gain will still need to be high enough to bring the X-ray events out of the noise, but low enough to work in the low combined shot noise regime.

3. EXPERIMENT

An uncoated, back-illuminated, e2v CCD97 shown in Figure 8 was taken to the BESSY II synchrotron for testing at a variety of X-ray energies in the range 0.2 to 1.2 keV. This facility was able to provide monochromatic photons with a controllable flux so that the device could be tested at a variety of energies and gains to look into the SNR improvement at different gains for a given energy. Spectra could be created so that the FWHM of the data could be assessed and the modified Fano factor at different low gains could be probed. The device was operated at -120 °C in non-inverted mode and the output was readout at 41 kHz. Images were acquired in full-frame, so that X-ray photons were incident during readout, reducing photon pileup and maximising the data collected per image.

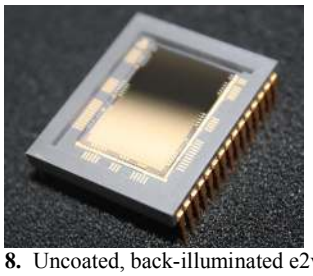

Figure 8. Uncoated, back-illuminated e2v CCD97

The EM-CCD was placed in a vacuum chamber and pumped down to a pressure of ~2E-6 mbar and then cooled to -120 °C. X-rays of a specified energy were targeted onto the chip using a pin-hole causing a 'trail' of electrons to be on left on the chip due to the readout of the device. 100 frames of 1 second integration were taken for each energy range to be analysed later. The data taken was:

Energy	1,200	1,000	800	600	400	280	200	150
Gain	1 & 7.76	1, 1.02, 1.3, 1.99, 4.77, 7.76, 14.69, 36.56	1 & 7.76	1 & 7.76	1 & 7.76	1, 1.99, 4.77, 7.76, 14.69, 36.56	1 & 7.76	1 & 7.76

Table 1. Gains and energies used at the BESSY synchrotron to evaluated EM-CCD behaviour.

This data allowed the modified excess noise factor to be investigated as well as showing the improvement possible in SNR and order separation and so the potential for the use of EM-CCDs on IXO could be evaluated.

4. RESULTS

Analysis of the results showed that, across all energies tested, the FWHM of the data varied from what should have been theoretically achieved, with discrepancy particularly obvious at low energies. Only data that came from isolated events have been considered at this time. In order to investigate this error a thresholding sensitivity study was completed and this showed that with a lower threshold the FWHM of the data improved, but the number of isolated events identified fell. The lower threshold caused some high level noise events to be considered as part of the X-ray event. Events that were isolated appeared to be split and so were ignored. In order to counter this effect a second threshold program was introduced.

A normal threshold of 5 sigma was applied to the data and this identified the isolated events. Then, using these positions as a frame of reference, a second threshold, just above the noise, was applied around these isolated events and any signal that was above this threshold was added into the isolated event and one average background value was subtracted. This produced a data set that was much closer to the theoretical values, but still contained enough events to be statistically significant.

One final data analysis tool was applied through the summation of all pixels around an isolated events and subtracting the appropriate number of average background events in an attempt to find all of the electrons produced by the X-ray events even when the electron production was only just above the noise.

4.1. Pixel summation

Low energy photons incident on the detector interacted close to the back-surface of the EM-CCD. The device was not deep-depleted and so the charge created by the X-ray event was able to drift in a large field-free region and this lead to splitting of the charge packet between neighbouring pixels (section 4.3). As thresholding proved to be poor at collecting all of the electrons generated by the X-ray interaction a pixel summation approach was considered.

When the signals of two pixels are added together off-chip (an example of off-chip binning) there is an increased level of apparent readout noise. This can be problematic for a conventional CCD because an increase in noise leads to a wider FWHM which makes it harder to achieve the order separation requirement, however, as an EM-CCD has gain that can be increased to reduce the equivalent readout noise to unity through signal amplification, the addition of extra readout noise has negligible impact and so pixel summation could prove to be a very powerful data analysis tool for low electron level soft X-ray photon detection. This method of pixel summation is described below.

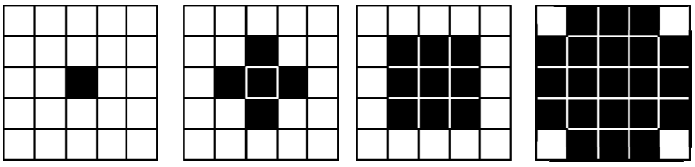

Figure 9. Pixel summation over 1, 5, 9 and 21 pixels about the central pixel.

Using a thresholding program, isolated events were identified and then the pixels surrounding them were summed into the isolated events after an average background value was subtracted. Several levels of summation were analysed, as shown by Figure 9, to see how close the data would come to the theory. This process showed that a very good FWHM that was close to the Fano limited theory could be achieved for high energies (~160 eV @ 1.2 keV). Splitting of events occurred at a level that was small causing some of the electrons generated by the X-ray to be lost through thresholding and so pixel summation regardless of threshold ensured all of the X-ray events was used.

The improvement at lower energies (< 600 eV) was more modest however and so suggests that either the splitting was over a greater distance than the level of summation that was analysed, or that some other process is causing a loss of charge. As the effect is prominent at lower energies, it is believed to be due to partial events from electron losses in the back-surface of the device as well as splitting due to the large free field region that the electrons could drift through.

The success of higher levels of summation over more than 21 pixels was limited due to the flux of the photons onto the device. By summing over larger numbers of pixels the potential of event pile-up increases, causing a high energy tail in the photo-peak and so degrading the FWHM. An optimal point between collecting the entire X-ray event and none of another was found to be at the 5 or 9 pixel summation level for the experimental flux.

4.2. Signal-to-noise ratio

The first thing that was noticed in the data was the difference in the SNR when looking at the data collected with a gain of 1 and a gain of 7. This is a small amount of gain compared to that traditionally applied with optical photons (>1,000). Using a small gain on the signal allows the modified Fano factor to be minimised and so the shot noise on both the detected signal and multiplication process has less of an effect on the FWHM of the X-ray photo-peak.

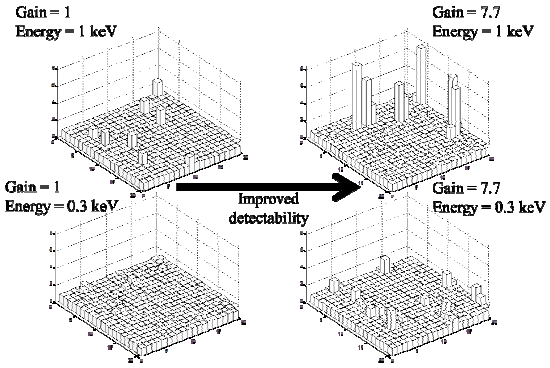

Figure 10. Data taken at BESSY with two different gains and energies. The top left image has an energy of 1.2 keV and a gain of 1, the bottom left image has an energy of 0.3 keV and a gain of 1. Both right hand images have a gain of ~7.7, with the top image having an energy of 1.2 keV and the bottom image and energy of 0.3 keV.

Figure 10 clearly shows the effect of using gain on the signal to noise ratio. With a gain of 1 at 1 keV the incident X-ray photons are clearly visible above the background noise of the device, but by introducing a gain of 7 they are immediately amplified and so become even more visible. This effect becomes more apparent at lower energies. At 300 eV, as only 82 electrons are produced by the incident photon, it is much harder to distinguish the charge packet above the background noise, the results have a poor signal to noise ratio and so many of the X-ray events will be lost. Again, by introducing a gain of 7, the X-ray events now become clearly visible above the noise. There is a large improvement in the signal to noise ratio and the events become much more visible above the noise and easier to detect. This helps to improve the Detection QE (DQE) which is a measure of the number of events that interact in the active silicon that can be detected above the noise in the device. This is not so much of a problem at high energies, but at the lower energies, maximising your SNR is important in order to detect as many of the X-rays as possible.

4.3. Split and partial events

On a back-illuminated EM-CCD the incident X-rays penetrate the back surface of the device and interact with the silicon. The generated electrons drift in the field-free silicon until they reach the depleted silicon and are then swept into a potential well underneath the electrode structure. At 300 eV, the interaction of the X-ray photon with the silicon will generate an average of 82 electrons. These electrons will be produced close to the back-surface of the device and will have a large thickness of field-free silicon to drift through. This causes the charge packet to drift under neighbouring potential wells and to be 'split' between pixels. As the number of electrons in the charge packet is small and the splitting between the adjacent pixels is high it is possible to lose some of the generated electrons into the noise through the thresholding of events.

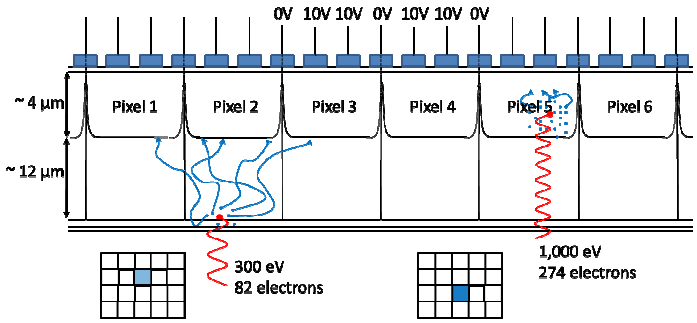

Figure 11. Showing how split events occur in silicon at varying X-ray energies.

A higher energy photon will not only penetrate further into the device before it interacts with the silicon, but will generate a larger number of electrons in the associated charge packet (1,000 eV photon will generate ~274 electrons). As the interaction occurs deeper into the device, the lateral drift in the field-free region of the device is smaller than for lower energies, or non-existent if the X-ray charge packet is generated entirely in a region of depleted silicon, and so a larger charge packet is shared between fewer pixels. An example of this is shown in Figure 11.

Partial events occur in the data due to the native oxide and 'dead' layer that are present in back-illuminated CCDs. If the incident photons do not have enough energy to pass through this layer then they will not be detected by the device. Figure 12 shows the transmission of X-ray photons through this dead layer and into the active silicon for the energy range required for the OP-XGS.

At 300 eV, 75 % of photons transmit through the un-responsive parts of the device and so 25 % of the incident photons are undetected. As the interaction between the X-ray and the silicon occurs very close to the back-surface of the device, some of the generated electrons will recombine with the silicon through recombination sites at the silicon-silicon dioxide interface. This will lead to incomplete charge collection and hence lead to partial events. These will manifest as a shift in the peak position of the X-ray event. By looking at where a low energy X-ray peak is compared with a calibration achieved with a high energy event, the new X-ray peak position can be found and so the reduction in energy calculated. This will give the partial event fraction.

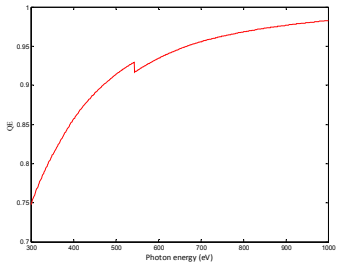

Figure 12. Modeled QE vs. against X-ray photon energy across the OPXGS energy band for an uncoated back-illuminated CCD.

4.4. The modified Fano-factor

The modified Fano factor is a measure of how much extra noise the shot noise on the multiplication register adds to the system. It is predicted to tend to 1.115, (1 + Fano factor) at high gain, but be smaller at lower gain (<10) following the behaviour of the excess noise factor with optical photons. It can be found by taking the equation to calculate the FWHM of a Gaussian distribution,

$$FWHM = 2\sqrt{2ln2}\sigma = 2.355\sigma$$

$$\sigma = \sqrt{\sigma_{readout}^2 + T(\sigma_{shot}^2) + \sigma_{dark}^2}$$

and re-arranging to make the modified Fano factor, T, the subject of this equation the values can be calculated, where $\sigma_{readout}$ is the readout noise, σ_{shot} is the shot noise and σ_{dark} is the dark current in the device. The results of this calculation are shown in Figure 13.

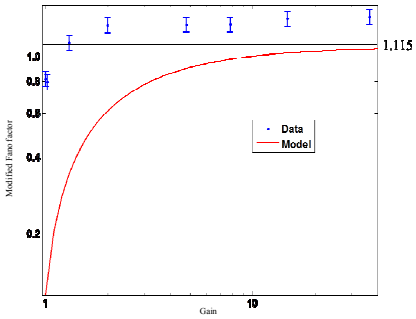

Figure 13. A plot comparing the modified Fano factor calculated from the data collected at BESSY (points) and the theoretical model developed from the EM-CCD Monte Carlo model (line)

Using the FWHM taken from the noise peak (this is the readout noise of the system) and the FWHM from the X-ray photo-peak to calculate the combined shot noise of the system the modified Fano factor of the system was calculated. The charge splitting of the X-ray events caused the data points to not be close enough to the line to verify the theory. However, it does show that the modified Fano factor tends to a value lower than 2 at high gain and so shows the effect that the Fano factor has on the total shot noise of an EM-CCD system and the possible improvement expected in terms of FWHM.

The greater distance seen between the theory and measured results at lower gain is expected, because the multiplied/amplified signal has a higher SNR, it is then easier to threshold the background noise out of the X-ray signal and collect a complete event more easily. Therefore the results achieved are closer to theory.

The values for the modified Fano factor still need to be verified, but these results clearly show that there is a definite dependence on gain with this signal in the low gain domain.

4.5. Order separation requirement results

The distance in energy needed to be resolved between adjacent orders for the OP-XGS is a minimum of 200 eV. By looking at the data for 400 eV and 600 eV X-rays shown in Figure 14, it is possible to see if this separation requirement is achieved.

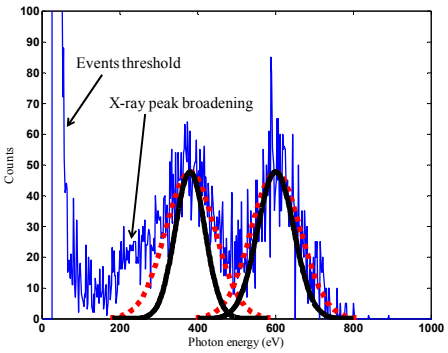

Figure 14. Histogram comparing position of 400 eV and 600 eV X-ray peaks. These peaks are fitted with Gaussians (dotted lines) and also with what the Gaussian would look like if the device performed as well as was theoretically possible (solid lines).

The 400 eV data show clear evidence of splitting and so a broadening of the peak, however, in the fitting of the Gaussian it is possible to ignore the extended effects of the split events. The 600 eV events are very closely fitted to the Gaussian (dotted line) which indicates a lower level of splitting. The dashed line Gaussians show that, while the peaks of the X-ray events are separate from each other, there is still a fair amount of cross-over that will confuse the data.

To see if the modified Fano factor would help with the order separation, secondary Gaussians were created and superimposed on the plot (solid lines). These show that the 400 eV X-ray peak has a lot of broadening away from theory, as would be expected for a low energy event in a device that wasn't fully depleted. The 600 eV theoretical Gaussian is much closer to the fitted Gaussian peak and so suggests that there is a lower level of splitting. Some of the split events have been programmed out of the data as the plots were created using pixel summation over 5 pixels.

The solid lines are clearly separated from each other and so achieve the order separation requirement that is needed in order to use EM-CCDs on the OP-XGS. This will only be possible, however, with the use of a deep depletion device.

5. CONCLUSIONS

Preliminary exploration of the use of EM-CCDs to detect X-rays and their applicability for use as the readout devices for the OP-XGS on IXO has been completed. A model has been presented for the excess noise of an EM-CCDs with soft X-rays at low gain and this has been tested with a campaign at BESSY. The increase in the modified Fano factor with increasing gain was a specific target of this test campaign in order to analyse how the FWHM of the X-ray peaks could be minimised. This is important in order for the EM-CCDs to be able to achieve the grating camera readout array order separation requirement.

Due to the large number of split events and partial events, pixel summation had to be used in order to collect as much of each X-ray event as possible. As pixels are added together the noise from each pixel is also added in quadrature. This leads to a degradation of the FWHM due to an increase in noise and so this has to be taken into account when looking at what is theoretically possible. When using a higher gain than 1 on the signal, the equivalent readout noise is suppressed and so the addition of extra readout noise, due to running at readout rates up to 5 MHz, may have minimal effect.

The pixel summation code had the desired effect at high energies where only a modest amount of pixel combination was necessary, however, at the lower energies the split events occurred over a much larger number of pixels due to absorption on the back surface and so larger summation schemes were necessary. Event pile-up meant that it was not possible to sum over as large an area as would have been necessary to collect the entire split event. Adjacent events would start to be included into the summation of the targeted event, leading to event confusion and a broadening to the X-ray peak towards higher energies.

Based on the theoretically model, using a deep depletion EM-CCD that is back-illuminated and has no AR coating would allow X-ray peaks with more signal in single peaks to be produced that have the necessary 200 eV separation and so meet the OP-XGS order separation requirement. This could be further enhanced through on-chip binning. EM-CCDs clearly make it possible to detect smaller signals with high detection efficiency, even with small gains and so should be considered for further the use on the OP-XGS on IXO.

REFERENCES

1. J. Bookbinder et al, "The International X-ray Observatory," *Activity submission in response to the Astro2010 RFI#2*, 2009.
2. R. L. McEntaffer et al., "X-ray performance of gratings in the extreme *off-plane* mount," *Proc. SPIE 5168,. 492-498, 2004*
3. A. Brinkman et al., "The Reflection Grating Spectrometer on board XMM," *Proceedings of the First XMM Workshop: Science with XMM", ESTEC, Noordwijk, The Netherlands, ed. M. Dahlem*
4. e2v technologies plc, " CCD97-00 Back-illuminated 2-Pjas IMO Series Electron Multiplying CCD Sensor," *e2v technologies plc datasheet A1A-CCD97BI_2P_IMO Issue 3,*. 2004
5. J. Geist & E.F. Zalewski., " The quantum yield of silicon in the visible," *Applied Physics Letters, Vol. 35, p. 503-505* 1979.
6. U. Fano., "On the theory of ionization yield of radiations in different substances," *Phys. Rev., 70 (1 & 2),* 1946
7. M. Robbins. et al, "The Noise Performance of Electron Multiplying Charge-Coupled Devices", *IEEE Transactions on Electron Devices 50(5), 1227-1232,* 2003
8. R. L. McEntaffer. et al, "Developments of the off-plane X-ray grating spectrometer for the International X-ray Observatory", Proc SPIE 7732-55, 2010